# AN OPTMIZED NaI(TL) MULTI-DETECTOR METHOD FOR THE DETERMINATION OF SPATIAL CONTAMINATION IN URBAN AREAS.

Instituto de Radioproteção e Dosimetria
CNEN - Brasil

Authors
– Marcos Cesar Ferreira Moreira (IRD-CNEN e UFRJ)
– Roberto Schirru (UFRJ)
– Claudio de Carvalho Conti (IRD-CNEN)

UNIVERSIDADE DO BRASIL

# Objectives

- **The objective of this work is to propose a system to assess the concentration of radioactive materials dispersed in a contaminated spatial urban or semi-urban environment in real time**
  - The proposed system could be used to either indicate contaminated hot spots and dose calculation in real time.

- **This system is based in:**
  - Use of three or four NaI(Tl) detectors asymmetrically shielded positioned 1m high above the ground of the studied environment;
  - Use of Monte Carlo Method to simulate the NaI(Tl) detector's response;
  - Artificial Neural Networks to trained with the simulated data set to quantify the contribution of each surface .

# Introduction

- **Contamination dynamics of urban and semi-urban surfaces by radioactive elements after either an intentional release or a nuclear/radiological accident:**
  - Complex modeling based on atmospheric dispersion models and deposition models - weather conditions.

- **Current status :**
  - In situ gamma-ray measurements;
  - Mathematical models to assess the dose at a given point in space due to contamination on surfaces;
  - Radioactive material distribution - on the surface, homogeneously distributed in the soil and distributed in the soil as a function of depth;
  - Single detector has been used, and the geometry of the source was an approach to a semi-infinite space with correction for finite geometry;

# Introduction

- **Single detector**
  - the spatial model of the urban surface contamination (wall, ground, roof etc.) is approached by the one-dimensional perception of the detector

- **Multiple detectors – Three-D approach and hot spot localization**
  - 3″ x 3″ NaI(Tl) four-detector cross -shaped layout asymmetrically shielded ;
  - 3″ x 3″ NaI(Tl) three-detector inverted-T layout asymmetrically shielded ;
  - The efficiency of a detector is greater in the unshielded area facing the surface;
  - The overall arrangement will be capable of identifying the photon's incidence angle based on the different response of each of the detectors to the incident photons;

# Introduction

- **Geometry complexity and random distribution of the contamination - No analytical method available**
- **Monte Carlo Method (MC) to simulate the response of each detector to contaminated surfaces - Monte Carlo N-Particle Code (MCNP5)**
- **Artificial Neural Networks (ANN):**
  - Use of the MC obtained data to study of several topologies of ANN;
  - Contamination assessment based on the response of each detector;

# Metodology

- Proof of concept based on a very simple case using only one $\gamma$ energy – 662 keV.
- Testing the linearity of the response of the detectors to different contamination concentration
- Obtaining suitable data sets to train and to test the pre-selected ANN's topologies, using the Monte Carlo Method to simulate the transport of photons
- Training of different Artificial Neural Networks topologies to solve the problem
- Optimizing the parameters – Detector's layout, shielding thickness, training data set (To better reflect the real case.)
- Studying the use of ANN in the energy range of interest – 50 keV to 3000 keV

# Related work – Proof of concept

## A New NaI(Tl) Four-Detector Layout for Field Contamination Assessment Using Artificial Neural Networks and the Monte Carlo Method for System Calibration

Published in April 07th, 2010 in the Nuclear Instruments and Methods in Physics Research – section A (doi:10.1016/j.nima.2010.04.027)

M. C. F. Moreira[1,2], C. C. Conti[1] and R. Schirru[2]

1 Universidade Federal do Rio de Janeiro, UFRJ/COPPE, Laboratório de Monitoração de Processos, P.O. Box 68509, 21941-972 Rio de Janeiro, Brazil

2 Instituto de Radioproteção e Dosimetria, CNEN/IRD, Av. Salvador Allende s/nº, P.O. Box 37750, 22780--160 Rio de Janeiro, Brazil

# Monte Carlo Method

- **“Solving particle transport problems with the Monte Carlo method is simple - just simulate the particle behavior.” LANL.**
- **The Monte Carlo method simulates the transport of photons or particles, following their individual paths based on the process of interaction of the photons with the matter.**
- **Monte Carlo Method simulate the history of a single particle from birth to death based on the generation of random numbers:**
  - Models collisions using physics equations & cross-section data;
  - Models free-flight between collisions using computational geometry;
  - Tallies the occurrences of events in each region;
  - Saves any secondary particles and analyzes them later.
- **MCNP5 – Is a Los Alamos NL well known and tested implementation of the MC Method**
  - Photons from 1 keV till 1 GeV
  - Follows 1e+09 photons per run

# Artificial Neural Networks – ANN

- Supervised networks - learn by example – adjust the weights
  - Feedforward, completely connected with 1, 2 or 3 hidden layers
  - Ward – 2 e 3 hidden layers connected from the input to the output – It uses Gaussian and complementary Gaussian to adjust different regions of the training data sets
- Learning algorithm – backpropagation
- Learning rate η e momentum α

$$w(n+1) = \alpha.\Delta w(n-1) - \eta.\Delta w(n) + w(n).$$

- Mean squared error – A statistical measure of the differences between the values of the outputs in the training set and the output values the network is predicting
- Stop criteria
  - Mean squared error = 1e-07
  - Number of epochs since the last mean squared error = 1e+05

# Experimental setup

- **Simple case study**
  - A model street composed of a wall on either side and the ground surface
- **Four 3"x3" NaI(Tl) detectors, 1 m above the ground and 5 m away from each wall.**
  - Dimensions:
    - Walls – 10m x 5 m;
    - Ground (street)– 10m x 10 m .
- **Cylindrical with 5cm thick lead shielding:**
  - One detectors facing each wall. No shielding in the surface of the detector facing the wall;
  - Two detectors facing the ground. No shielding in the bottom

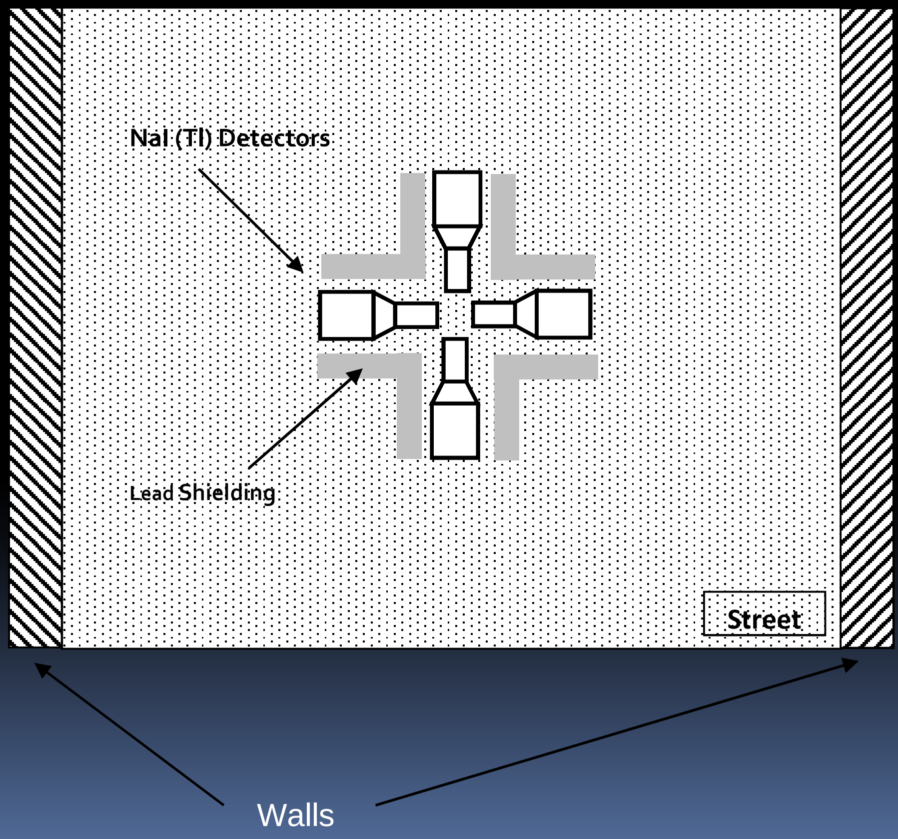

# Proposed four-detector layout

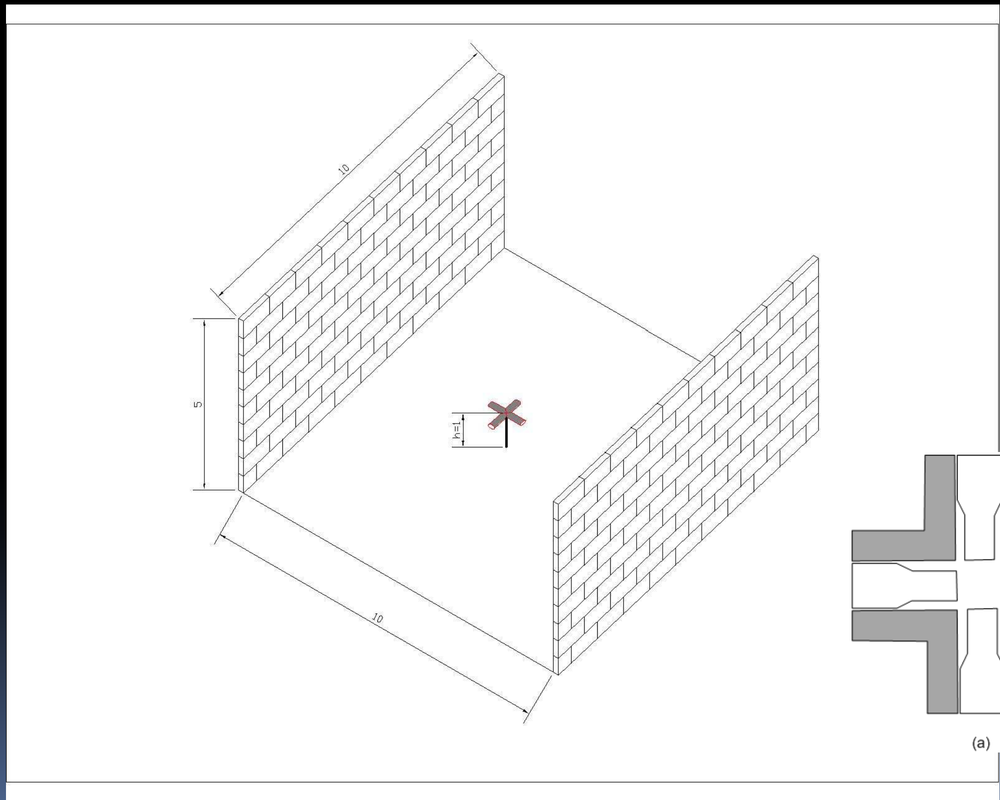


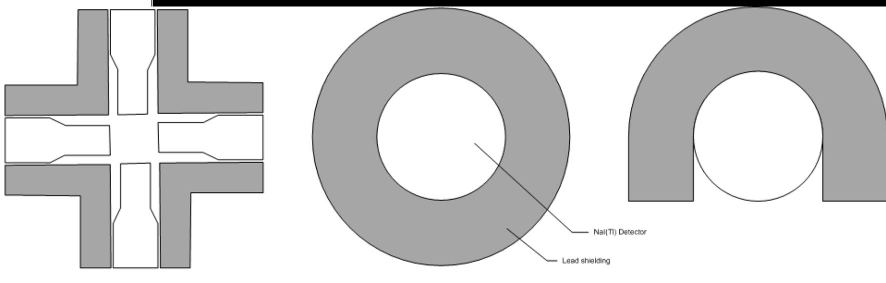


(a) (b) (c)

# Proposed three-detector layout

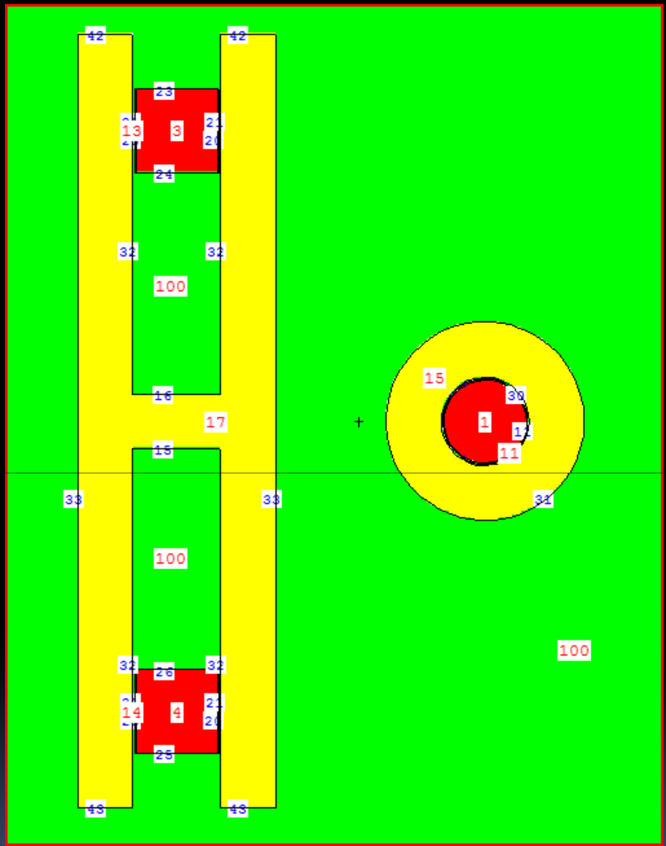


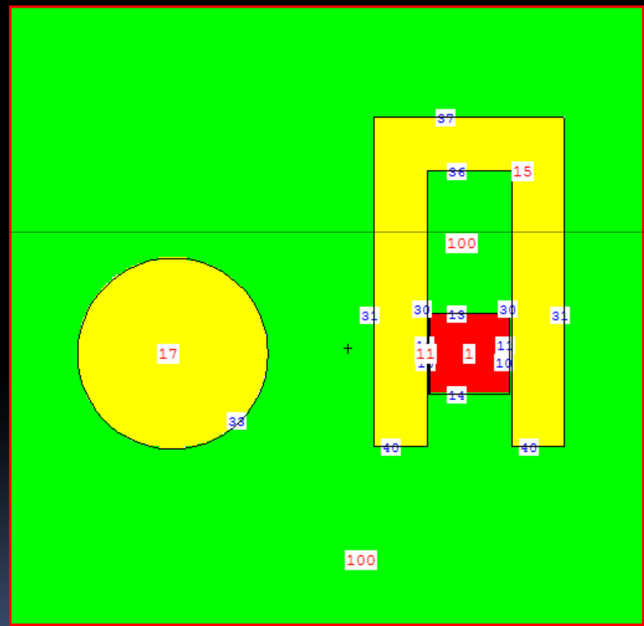

# Testing the Linearity of the detectors' response

- Testing the linearity with respect to the variation of the photons concentration in each surface:
  - It was obtained the response of each of the four detectors, using the MCNP5, for the concentrations of 1e+05, 1e+06, 1e+07, 1e+08, 1e+09 and 8e+09 $\gamma.m^{-2}$ in each surface for the energies of 662 keV:
- No photons reached the detectors for surface concentration values lower than 1e+05 $\gamma.m^{-2}$
- The code follows 1e+09 photons per run, to obtain the results to higher values the surfaces were divided into eighths with 1e+09 $\gamma.m^{-2}$ in each and summed up.

# Linearity of the detectors' response

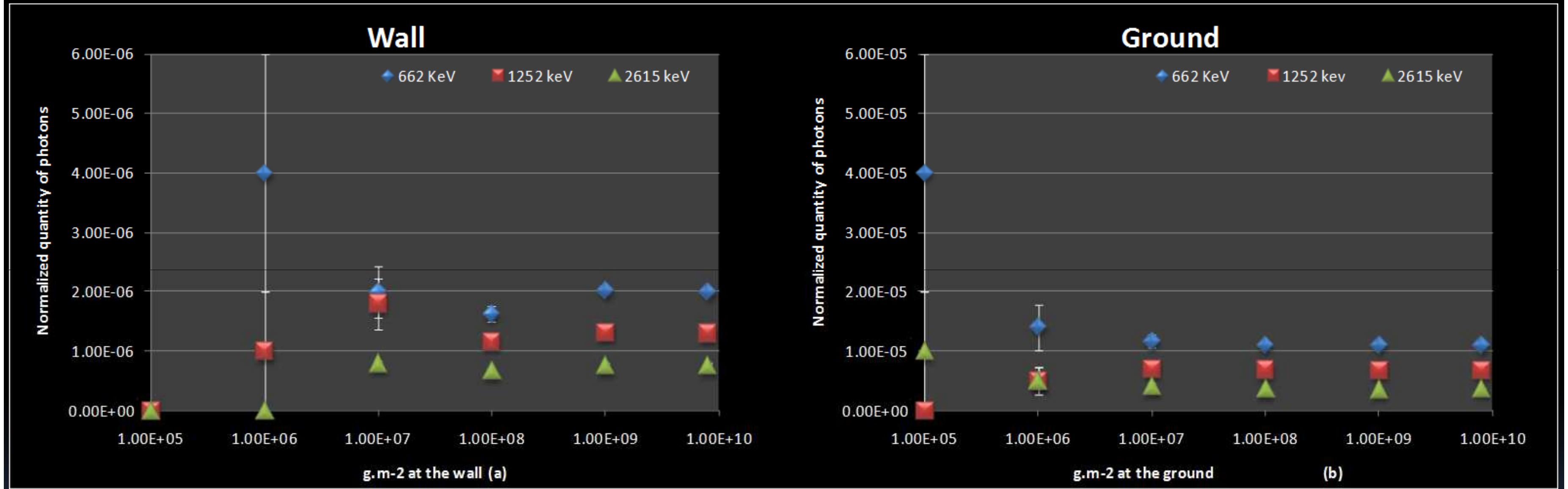


The proportionality of the response could be used to derive other data sets to train the ANNs.

# Detectors' response and training data sets

- Response of each detector to contamination of the three areas.
  - Based on the verified linearity of the response, it was defined the ranges of contamination of surfaces up to 8e+09 $\gamma.m^{-2}$.
  - Training used values -> 0, 1e+07, 5e+07, 1e+08, 5e+08, 1e+09 e 8e+09 $\gamma.m^{-2}$.
  - Counting values were calculated for the four detectors.
  - For values below 1e+07 $\gamma.m^{-2}$, due to low statistical detection, error values were high. Therefore, values below that value were not used.
  - The highest value obtained through simulation was 8e+09 $\gamma.m^{-2}$ per surface.
  - The training data sets were obtained by combining the above values of contamination on each surface.
    - 345 elements with 3 input variables (walls and ground) and 3 or 4 output values (counting at the studied energy at each detector).

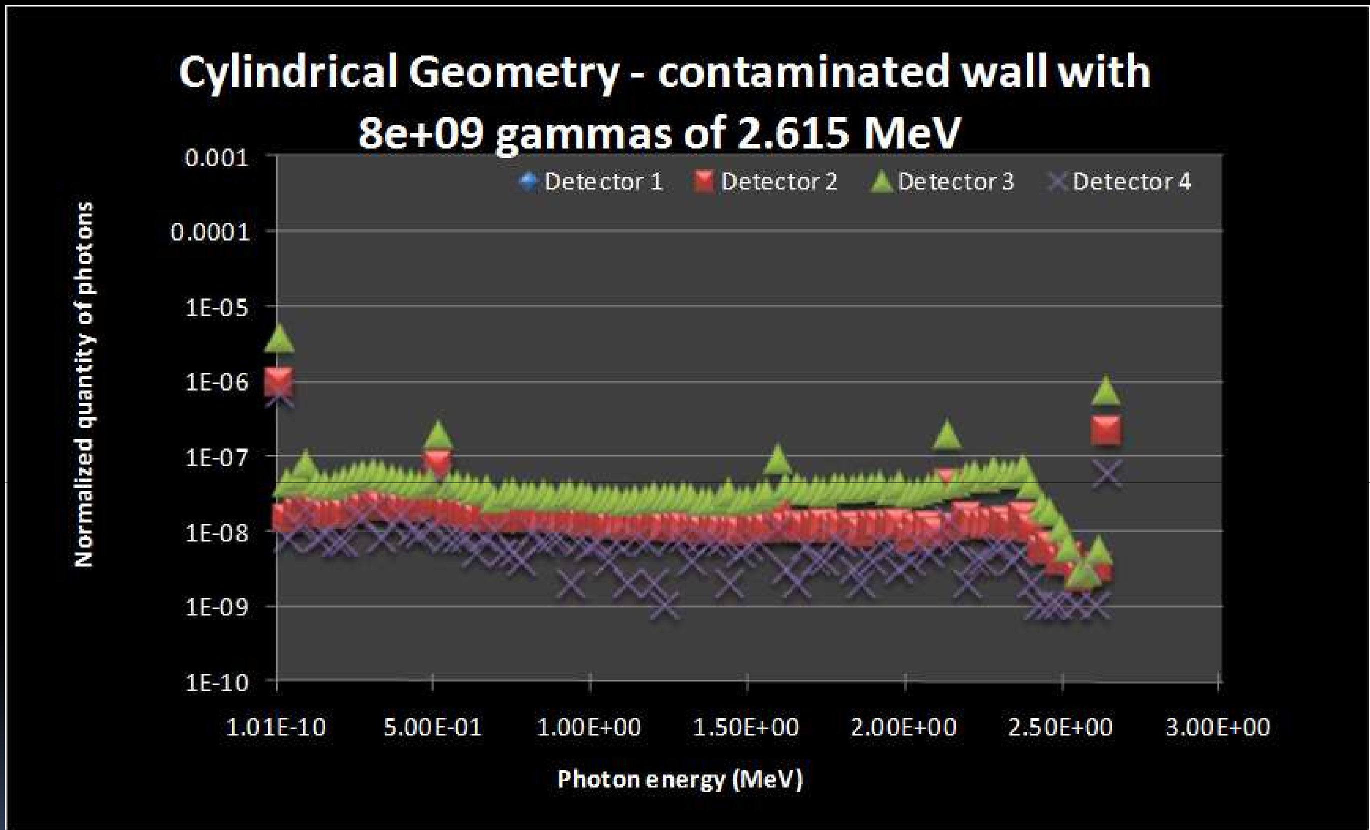


2.615 keV spectrum obtained with Monte Carlo Method simulation

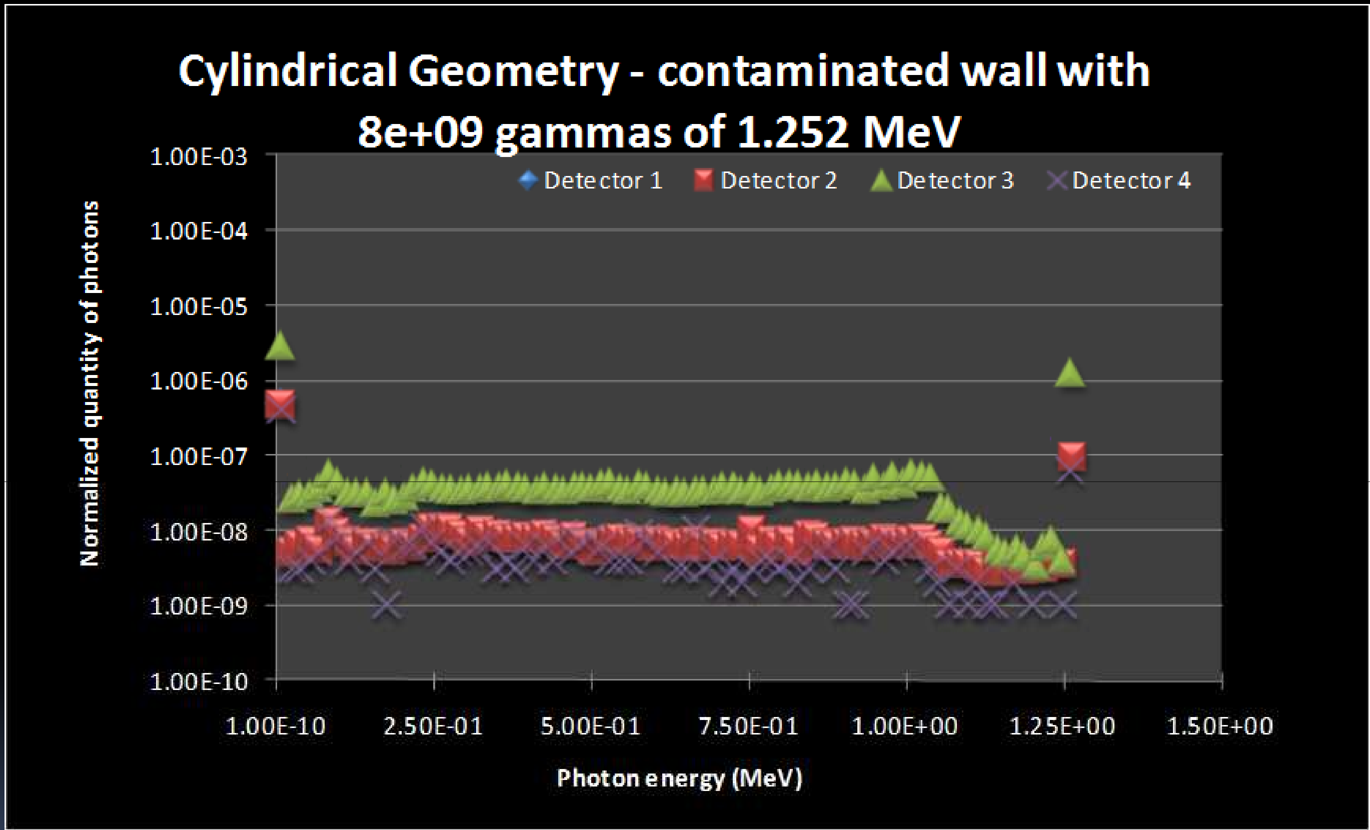


1.252 keV spectrum obtained with Monte Carlo Method simulation

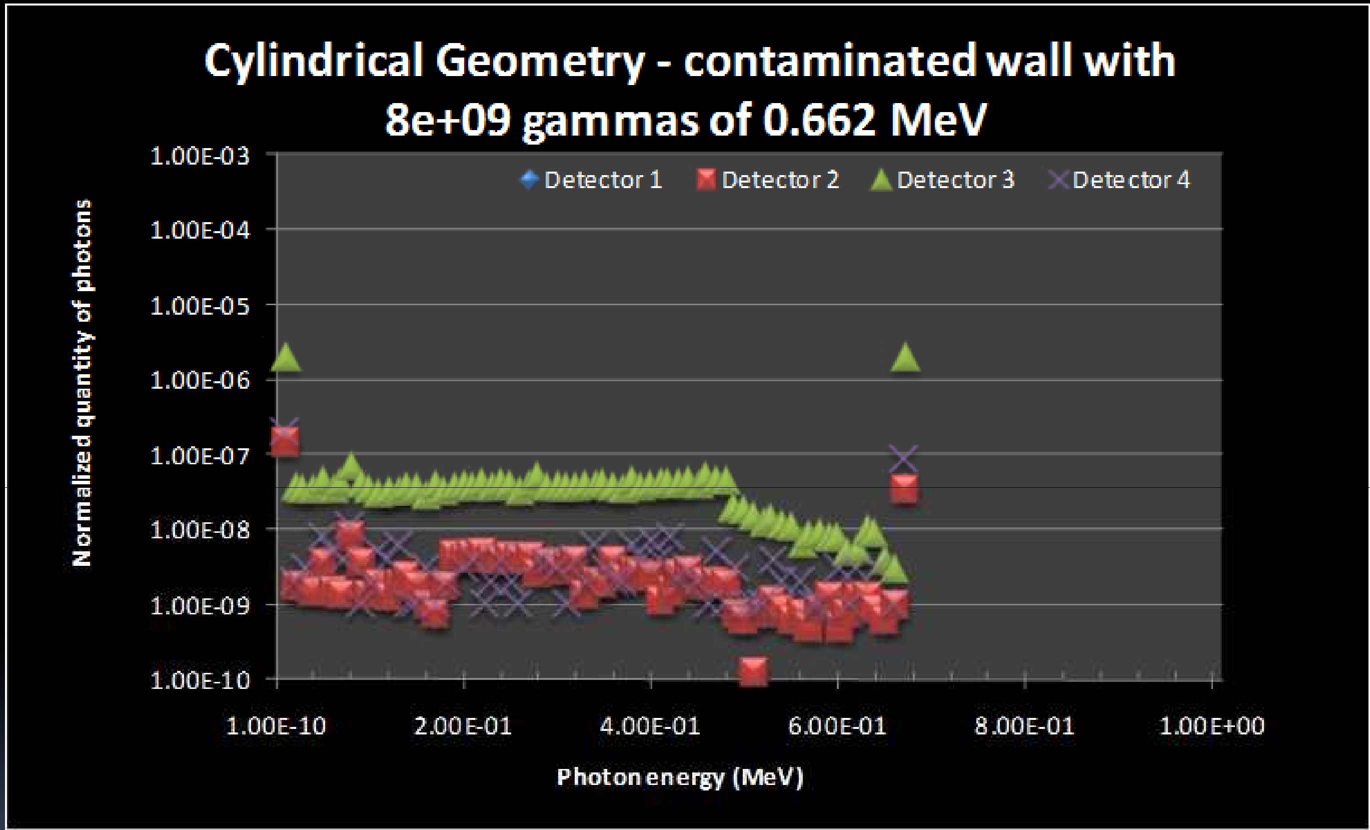


662 keV spectrum obtained with Monte Carlo Method simulation

# Artificial Neural Networks
## training and testing

- Pre-selection of topologies of ANNs to study.
- Evaluation of training outcomes and choice of ANN's that showed better results in terms of :
  - $R^2$ - coefficient of multiple determinations
  - r - correlation coefficient and $r^2$ - Coefficient of determination
- Test of these networks with two production data sets for the energy of 662 keV and choose the best candidate: :
  - Data set 1
    - Values within the trained data set range.
    - Values - from 1e+7 to 1e+10 $\gamma.m^{-2}$.
  - Data set 2
    - Values inside and outside the trained data set range;
    - Values - from 0 to 1e+10 $\gamma.m^{-2}$.
- Additional test of the chosen ANN for the energies of 1252 keV e 2615 keV.

# Table 1 – Artificial neural network topologies, training time, and mean squared errors.

| | Layer 1 | Layer 2 | Layer 3 | Layer 4 | Layer 5 | Error[a] |
|---|---|---|---|---|---|---|
| **case 1[b]** | **tanh 4** | **logistic 20** | **logistic 3** | | | **1,00E-07** |
| case 2 | tanh 4 | logistic 50 | logistic 3 | | | 2,00E-07 |
| case 3 | tanh 4 | logistic 100 | logistic 3 | | | 1,00E-07 |
| case 4 | tanh 4 | logistic 10 | logistic 10 | logistic 3 | | 1,60E-06 |
| case 5 | tanh 4 | logistic 20 | logistic 20 | logistic 3 | | 1,50E-01 |
| case 6 | tanh 4 | logistic 7 | logistic 7 | logistic 7 | logistic 3 | 1,40E-06 |
| **case 7[b]** | **tanh 4** | **logistic 20** | **logistic 20** | **logistic 20** | **logistic 3** | **1,00E-07** |
| **case 8[b]** | **tanh 4** | **logistic 40** | **logistic 40** | **logistic 3** | | **1,00E-07** |
| **case 9[b]** | **tanh 4** | **logistic 40** | **logistic 40** | **logistic 40** | **logistic 3** | **1,00E-07** |
| case 10 | tanh 4 | Gaussian 10 (ward) | Gaussian 10 com(ward) | logistic 3 | | 2,40E-05 |
| **case 11[b]** | **tanh 4** | **Gaussian 20 (ward)** | **Gaussian 20 com(ward)** | **logistic 3** | | **1,00E-07** |
| case 12 | tanh 4 | Gaussian 40 (ward) | Gaussian 40 com(ward) | logistic 3 | | 1,00E-07 |
| case 13 | tanh 4 | Gaussian 7 (ward) | Gaussian 7 com(ward) | tanh 7 | logistic 3 | 7,00E-07 |
| **case 14[b]** | **tanh 4** | **Gaussian 20 (ward)** | **Gaussian 20 com(ward)** | **tanh 20** | **logistic 3** | **1,00E-07** |
| **case 15[b]** | **tanh 4** | **Gaussian 40 (ward)** | **Gaussian 40 com(ward)** | **tanh 40** | **logistic 3** | **1,00E-07** |
| case 16 | tanh 4 | Gaussian 10 (ward) | Gaussian 10 com(ward) | logistic 3 | (Jump) | 5,00E-07 |
| case 17 | tanh 4 | Gaussian 20 (ward) | Gaussian 20 com(ward) | logistic 3 | (Jump) | 3,00E-07 |
| case 18 | tanh 4 | Gaussian 20 (ward) | Gaussian 20 com(ward) | logistic 3 | (Jump) | 4,00E-07 |

Learning rate = 0.5 Momentum = 0.6

a Cases 1 – 9 simple feed forward networks.
Cases10–18WARDnetworks.

b Mean squared error.

C Training stopped by the mean squared error criterion or when 100,000 epochs occurred after last min or mean squared error.

# Table 2 – $R^2$, $r^2$ and correlation coefficient for the ANN's.

| | $R^2$ | | | $r^2$ | | | Correlation coefficient | | |
|---|---|---|---|---|---|---|---|---|---|
| | Wall | | | Wall | | | Wall | | |
| | Left | Right | Ground | Left | Right | Ground | Left | Right | Ground |
| Case 1 | 0 | 0 | 0 | 0,0426 | 0,0239 | 0,0884 | 0,2064 | 0,1546 | 0,2974 |
| **Case 2** | **1** | **1** | **1** | **1** | **1** | **1** | **1** | **1** | **1** |
| **Case 3** | **1** | **1** | **1** | **1** | **1** | **1** | **1** | **1** | **1** |
| **Case 4** | **1** | **1** | **1** | **1** | **1** | **1** | **1** | **1** | **1** |
| **Case 5** | **1** | **1** | **1** | **1** | **1** | **1** | **1** | **1** | **1** |
| Case 6 | 0 | 0 | 0 | 0,1887 | 0,1833 | 0,1019 | 0,4344 | 0,4282 | 0,3191 |
| **Case 7** | **1** | **1** | **1** | **1** | **1** | **1** | **1** | **1** | **1** |
| Case 8 | 0 | 0 | 0 | 0,2015 | 0,2163 | 0,074 | 0,4488 | 0,465 | 0,272 |
| **Case 9** | **0** | **0** | **0** | **0,1889** | **0,182** | **0,0195** | **0,4346** | **0,4267** | **0,1396** |
| Case 10 | 0,9999 | 0,9998 | 0,9999 | 0,9999 | 0,9998 | 0,9999 | 0,9999 | 0,9999 | 1 |
| **Case 11** | **1** | **1** | **1** | **1** | **1** | **1** | **1** | **1** | **1** |
| Case 12 | 0 | 0 | 0 | 0,0011 | 0,0009 | 0,0009 | 0,0326 | 0,0304 | 0,0305 |
| **Case 13** | **1** | **1** | **1** | **1** | **1** | **1** | **1** | **1** | **1** |
| **Case 14** | **1** | **1** | **1** | **1** | **1** | **1** | **1** | **1** | **1** |
| **Case 15** | **1** | **1** | **1** | **1** | **1** | **1** | **1** | **1** | **1** |
| **Case 16** | **1** | **1** | **1** | **1** | **1** | **1** | **1** | **1** | **1** |
| Case 17 | 0 | 0 | 0 | 0,2063 | 0,2259 | 0,1459 | 0,4542 | 0,4752 | 0,3819 |
| Case 18 | 0 | 0 | 0 | 0,1656 | 0,1596 | 0,0009 | 0,4069 | 0,3995 | 0,0305 |

Table 3 – $R^2$, $r^2$ and correlation coefficient for the ANN´s 7, 14, 11 e 15, for the energy 662 keV using the training and production data sets.

| | | $R^2$ | | | $r^2$ | | | Coeficiente de correlação | | |
|---|---|---|---|---|---|---|---|---|---|---|
| | | Wall | | | Wall | | | Wall | | |
| | | Left | Right | Ground | Left | Right | Ground | Left | Right | Ground |
| Training data set | case 7 | 1,0000 | 1,0000 | 1,0000 | 1,0000 | 1,0000 | 1,0000 | 1,0000 | 1,0000 | 1,0000 |
| | case 11 | 1,0000 | 1,0000 | 1,0000 | 1,0000 | 1,0000 | 1,0000 | 1,0000 | 1,0000 | 1,0000 |
| | **case 14** | **1,0000** | **1,0000** | **1,0000** | **1,0000** | **1,0000** | **1,0000** | **1,0000** | **1,0000** | **1,0000** |
| | case 15 | 1,0000 | 1,0000 | 1,0000 | 1,0000 | 1,0000 | 1,0000 | 1,0000 | 1,0000 | 1,0000 |
| Production data set (inside trained range) | case 7 | 0,9986 | 0,9993 | 0,9984 | 0,9991 | 0,9995 | 0,9996 | 0,9995 | 0,9998 | 0,9998 |
| | case 11 | 0,4952 | 0,9871 | 0,9969 | 0,7331 | 0,9882 | 0,9988 | 0,8562 | 0,9941 | 0,9994 |
| | **case 14** | **0,9999** | **0,9998** | **0,9994** | **0,9999** | **0,9999** | **0,9999** | **1,0000** | **1,0000** | **0,9999** |
| | case 15 | 0,8043 | 0,9814 | 0,9775 | 0,8535 | 0,9819 | 0,9937 | 0,9239 | 0,9909 | 0,9969 |
| Production data set (outside trained range) | case 7 | 0,0000 | 0,0762 | 0,3275 | 0,7433 | 0,6507 | 0,9042 | 0,8621 | 0,8066 | 0,9509 |
| | case 11 | 0,1036 | 0,0765 | 0,0464 | 0,3374 | 0,3222 | 0,6569 | 0,5808 | 0,5676 | 0,8105 |
| | case 14 | 0,1146 | 0,0725 | 0,0464 | 0,3479 | 0,2798 | 0,6527 | 0,5898 | 0,5290 | 0,8079 |
| | case 15 | 0,1056 | 0,0764 | 0,0464 | 0,3593 | 0,3129 | 0,6568 | 0,5994 | 0,5593 | 0,8104 |

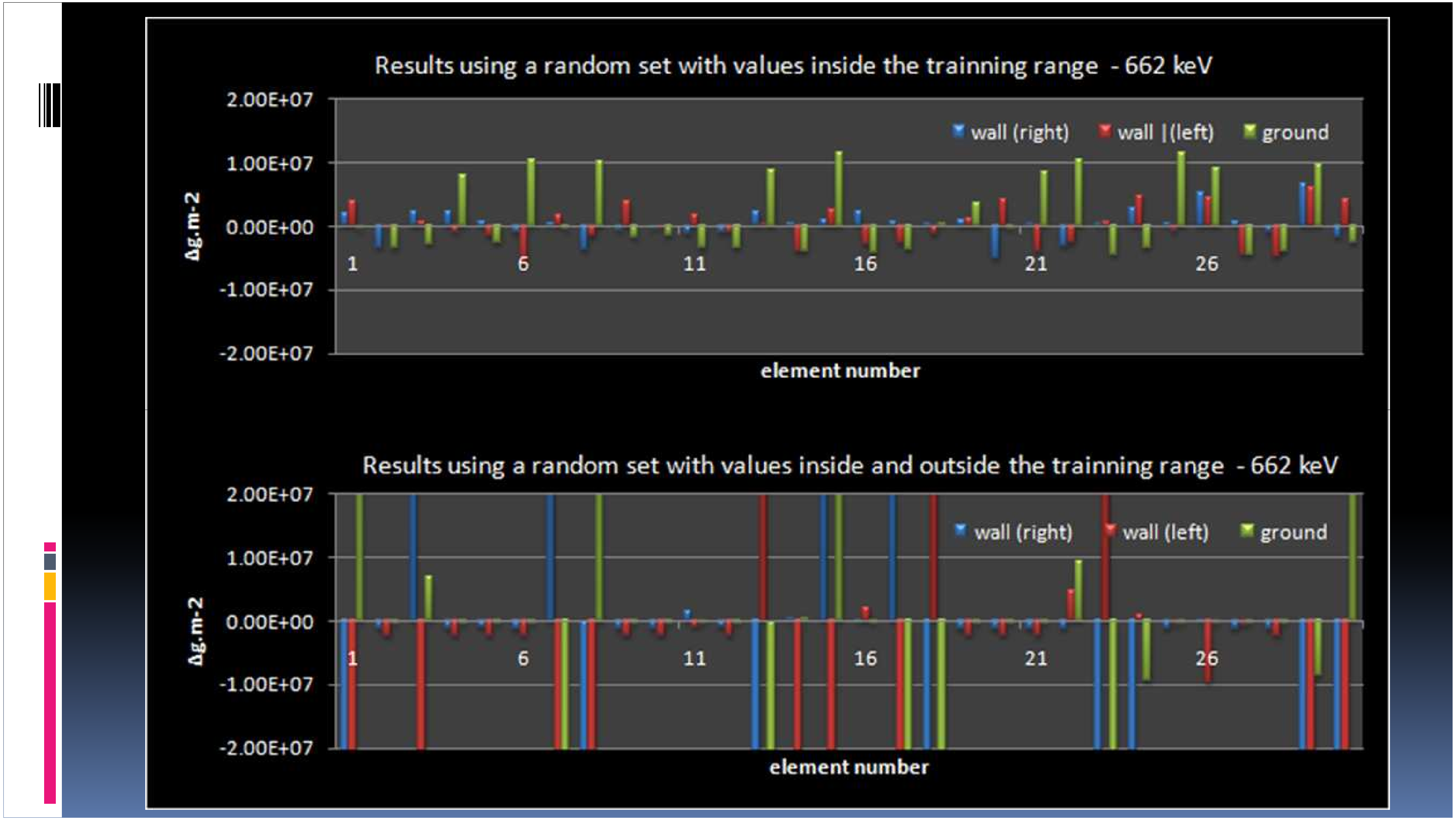
Results using a random set with values inside the trainning range - 662 keV
2.00E+07
1.00E+07
0.00E+00
-1.00E+07
-2.00E+07
Δg.m-2
wall (right)
wall |(left)
ground
1
6
11
16
21
26
element number
Results using a random set with values inside and outside the trainning range - 662 keV
2.00E+07
1.00E+07
0.00E+00
-1.00E+07
-2.00E+07
Δg.m-2
wall (right)
wall (left)
ground
1
6
11
16
21
26
element number

Table 4 – $R^2$, $r^2$ e Correlation coefficient for the ANN 14, for the training and production data sets for the energies of 662 keV, 1252 keV and 2615 keV.

| | | $R^2$ | | | $r^2$ | | | Coeficiente de correlação | | |
|---|---|---|---|---|---|---|---|---|---|---|
| | | Wall | | | Wall | | | Wall | | |
| | Energy | Left | Right | Ground | Left | Right | Ground | Left | Right | Ground |
| Training set | 662 KeV | 1,0000 | 1,0000 | 1,0000 | 1,0000 | 1,0000 | 1,0000 | 1,0000 | 1,0000 | 1,0000 |
| | 1252 KeV | 1,0000 | 1,0000 | 1,0000 | 1,0000 | 1,0000 | 1,0000 | 1,0000 | 1,0000 | 1,0000 |
| | 2615 keV | 1,0000 | 1,0000 | 1,0000 | 1,0000 | 1,0000 | 1,0000 | 1,0000 | 1,0000 | 1,0000 |
| Production set (inside range) | 662 KeV | 0,9999 | 0,9998 | 0,9994 | 0,9999 | 0,9999 | 0,9999 | 1,0000 | 1,0000 | 0,9999 |
| | 1252 KeV | 0,9998 | 0,9997 | 0,9995 | 0,9999 | 0,9999 | 0,9998 | 0,9999 | 0,9999 | 0,9999 |
| | 2615 keV | 0,9997 | 0,9998 | 0,9998 | 0,9999 | 0,9999 | 1,0000 | 0,9999 | 1,0000 | 1,0000 |
| Production set (outside range) | 662 KeV | 0,1146 | 0,0725 | 0,0464 | 0,3479 | 0,2798 | 0,6527 | 0,5898 | 0,5290 | 0,8079 |
| | 1252 KeV | 0,0444 | 0,0511 | 0,0000 | 0,1756 | 0,1525 | 0,6921 | 0,4190 | 0,3906 | 0,8319 |
| | 2615 keV | 0,0000 | 0,2006 | 0,0543 | 0,5034 | 0,2924 | 0,3168 | 0,7095 | 0,5407 | 0,5628 |


Results using the training data set - 662 keV
Parede (direita)
Parede (esquerda)
Solo
Δγ.m-2
Data set element
Results using the training data set - 1252 keV
Parede (direita)
Parede (esquerda)
Solo
Δγ.m-2
Data set element
Results using the training data set - 2615 keV
Parede (direita)
Parede (esquerda)
Solo
Δγ.m-2
Data set element

Table 5 – $R^2$, $r^2$ e Correlation coefficient for the **three-detector** layout using the ANN 14, for the training and production data sets for the energy of 662 keV.

| shielding | | 2.5 cm | | | 5 cm | | | 7.5 cm | | | 10 cm | | |
|---|---|---|---|---|---|---|---|---|---|---|---|---|---|
| | | Detector 1 | Detector 2 | Detector 3 | Detector 1 | Detector 2 | Detector 3 | Detector 1 | Detector 2 | Detector 3 | Detector 1 | Detector 2 | Detector 3 |
| Training data set | $R^2$ | 1.0000 | 1.0000 | 1.0000 | 1.0000 | 1.0000 | 1.0000 | 1.0000 | 1.0000 | 1.0000 | 1.0000 | 1.0000 | 1.0000 |
| | $r^2$ | 1.0000 | 1.0000 | 1.0000 | 1.0000 | 1.0000 | 1.0000 | 1.0000 | 1.0000 | 1.0000 | 1.0000 | 1.0000 | 1.0000 |
| | r | 1.0000 | 1.0000 | 1.0000 | 1.0000 | 1.0000 | 1.0000 | 1.0000 | 1.0000 | 1.0000 | 1.0000 | 1.0000 | 1.0000 |
| Production data set (inside) | $R^2$ | 0.9921 | 0.9376 | 0.9996 | 0.9840 | 0.9984 | 0.9988 | 0.9834 | 0.9901 | 0.9983 | 0.9534 | 0.9892 | 0.9979 |
| | $r^2$ | 0.9934 | 0.9581 | 0.9998 | 0.9853 | 0.9987 | 0.9991 | 0.9907 | 0.9953 | 0.9994 | 0.9776 | 0.9952 | 0.9992 |
| | r | 0.9967 | 0.9788 | 0.9999 | 0.9926 | 0.9994 | 0.9996 | 0.9954 | 0.9976 | 0.9997 | 0.9887 | 0.9976 | 0.9996 |
| Production data set (outside) | $R^2$ | 0.0000 | 0.0000 | 0.0950 | 0.0000 | 0.0678 | 0.0220 | 0.1476 | 0.0393 | 0.1719 | 0.0000 | 0.0000 | 0.0119 |
| | $r^2$ | 0.3779 | 0.0195 | 0.1843 | 0.2622 | 0.2602 | 0.4004 | 0.6822 | 0.4103 | 0.4338 | 0.4172 | 0.5205 | 0.4591 |
| | r | 0.6148 | 0.1395 | 0.4293 | 0.5121 | 0.5101 | 0.6328 | 0.8260 | 0.6405 | 0.6586 | 0.6459 | 0.7215 | 0.6776 |

# Conclusions

- The use of the Monte Carlo calculations in combination with artificial neural networks has been proven to be an adequate tool to calibrate detectors' system for highly complicated detection geometries.
- The four-detector and the three-dector 3"x3" NaI(Tl) layout had proven to be adequate, calibrate with this method, to determine the spatial contamination in urban and semi-urban areas.
- Several ANN topologies have responded accurately to the values of the training data set and also to a production data set of value within the range of the trained values.
- Lead shielding of 5 an 7.5 cm showed better results, and can be used.

# Conclusions

- Within the range of the training data set, one of the proposed network topologies (case 14) can be used to predict the values of concentration of the photons on the surfaces based on the number of photons that reach each one of the target detectors.
- Results show that the problem dealt within this paper is indeed very complex and that generalization outside the training range could not be achieved at all, as shown by the results with the production set with values outside this range. Therefore, the training data set should be chosen to best represent the expected range of number of photons emerging from the contaminated surface.

# Next steps

- **Study of this work to the energy range of interest ( up to 3000 keV) – test all the pre-selected ANN topologies in this range**
- **Study of hot spot localization – angle of incidence**
  - Select an adequate detector layout;
  - Generate the data sets; and
  - train ANNs to indicate the angle and the distance of a hot spot

Thank you!

# References


- **Conti, C. C., et al. 2000.** Air Kerma Above Environmental Radiometric Calibration Facility For field Equipmant. *V Encontro Nacional de Aplicações Nucleares.* 2000.
- **—. 1999.** Ge Detectors calibration procedure at IRD/CNEN for in situ measurements. *Internationational Symposium on Technologiically Enhanced Natural Radiation.* 1999.
- **Fausett, L V. 1994.** *Fundamentals of Neural Networks`Architeture, Algorithms and Applications.* s.l. : Prentice Hall, 1994.
- **Hendricks, P. H. G. M., Mau, M. e Meijer, R. J. 2002.** MCNP Modelling of Scintillation-Detector Gamma-Ray Spectra From Natural Nuclides. *Applied Radiation and Isotopes.* 2002, Vol. 57, pp. 449-457.
- **Jacob, P. e Meckbach, R. 1987.** Shielding Factors and External Dose Evaluation. *Radiation Protection Dosimetry.* 1987, Vols. 21, n.1-3, pp. 79-85.
- **Jacob, Peter e Paretzke, Herwig G. 1986.** Gamma-ray exposure from contaminated soil. *Nuclear Science and Engineering.* 1986, Vol. 93.

# References


- **Kalos, M. H. e Whitlock, P. A. 1986.** *Monte Carlo Methods.* New York : Wiley - Interscience publication, 1986.
- **Knoll, Glenn F. 1979.** *Radiation Detection and Mesaurement.* New York : John Wiley and Sons Inc., 1979. ISBN 0-471-49545-X.
- **Los Alamos national Laboratory. 2003.** MCNP - A General Monte Carlo n-particle transporte code: Overview and theory. 2003.
- **Moreira, Marcos C. F. 1990.** Padronização de um método para espectrometria gama in situ com detector de Germânio. *Dissertação de Mestrado, M.Sc.* Rio de Janeiro, RJ, Brasil : COPPE - UFRJ, 1990.
- **Rieppo, R e Vanska, R. 1978.** Efficiency Calibration of a 4" x 4" face-type NaI(Tl) doble crystal gamma-ray spectrometer. *Nuclear Instruments and Methods.* 1978, Vol. 155, Issue 3, pp. 459-465.
- **Rubinstein, R. Y. 1981.** *Simulation and the Monte Carlo Method.* New York : John Wiley & Sons, Inc., 1981.

# References


- **Sachett, Ivanor A. 2002.** Caracterização da radiação gama ambiental em área urbana usando uma unidade móvel de rastreamanto. *Tese de Doutorado, D.Sc.* Rio de Janeiro, RJ, Brasil : IBRAG - UERJ, 2002.
- **Saito, K e Moriuchi, S. 1981.** Monte Carlo Calculation of accurate response functions for a NaI(Tl) detector for gamma rays. *Nuclear Instruments and Methods.* 1981, Vol. 185, pp. 299-308.
- **Salinas, I. C. P., Conti, C. C. e Lopes, R. T. 2006.** Effective Density and Mass Attenuation Coeficient for Building Material in Brazil. *Applied Radiation and Isotopes.* 2006, Vol. 64, pp. 13-18.
- **Salinas, Isabel C. P. 2006.** Determinação dos fatores de blindagem para construções tipicamente brasileiras. [ed.] UFRJ - COPPE. *Tese de Doutorado, D.Sc.* Rio de Janeiro, RJ, Brasil : s.n., 2006.
- **Ward Systems Group Inc. 1993.** NeuroShell II Manual. 1993.